CROP BREEDING AND APPLIED BIOTECHNOLOGY

*ARTICLE*

# QTL mapping for Type II resistance to Fusarium head blight and spike architecture traits in bread wheat

Crop Breeding and Applied Biotechnology
22(2): e38242229, 2022
Brazilian Society of Plant Breeding.
Printed in Brazil
http://dx.doi.org/10.1590/1984-70332022v22n2a19

**Maria Fiorella Franco[1,2], Gladys Albina Lori[3,4], Maria Gabriela Cendoya[1], Juan Panelo[1], María Pía Alonso[1,2], Ismael Malbrán[2,4] and Ana Clara Pontaroli[1,2*]**

**Abstract:** *In breeding for resistance to Fusarium head blight (FHB) there should be precise differentiation between QTL for resistance and those for spike architecture traits that indirectly affect disease. QTL mapping for FHB Type II resistance and spike architecture traits was carried out in a population of 80 RIL. Three QTL for FHB Type II resistance were identified respectively on chromosomes 2A, 4A and 6D, the last of which is reported here for the first time. The number of florets per spike and per spikelet was associated with FHB Type II resistance but there was not co-localization between QTL for these traits. However, QTL for number of spikelets per spike overlapped with those for FHB Type II resistance on chromosomes 2A and 6D. Spike architecture traits - notably, the number of florets per spike and per spikelet - should be considered in the design of breeding strategies to increase Type II resistance to FHB in bread wheat.*

**Keywords**: *Triticum aestivum L.,* quantitative trait loci, disease severity, area under the disease progress curve, spike morphology

## INTRODUCTION

Fusarium head blight (FHB), caused by several species of the *Fusarium* genus (mainly *Fusarium graminearum*), is a devastating disease of bread wheat (*Triticum aestivum* L.) in environments with prolonged wet climatic conditions from flowering through the soft-dough stage of kernel development (Bai et al. 2018). This destructive disease leads to severe losses in yield and quality and to contamination with fungal mycotoxins in the grains, which render them unsuitable for human or animal consumption (Ferrigo et al. 2016, Mielniczuk and Skwaryło-Bednarz 2020).

Due to the limited success of agronomic practices in reducing the impact of FHB, genetic resistance is the most effective and consistent strategy for diminishing the losses caused by the disease (CIMMYT 2019). Resistance to FHB is a complex trait, quantitatively inherited. The infection and the development of the disease are highly influenced by the environment, and the strong genotype-by-environment interaction reduces the accuracy of disease assessments (Steiner et al. 2017). Fusarium Head Blight resistance is divided mainly into resistance to initial infection (Type I) and resistance to spread of the fungus within spikes after infection (Type II) (Mesterhazy 2020). Likewise, both active and passive resistance mechanisms contribute to FHB resistance. Active

***Corresponding author:**
E-mail: pontaroli.ana@inta.gob.ar
*ORCID: 0000-0002-2605-7668*

**Received:** 20 May 2021
**Accepted:** 31 January 2022
**Published:** 31 May 2022

[1] 1 Unidad Integrada Balcarce (Facultad de Ciencias Agrarias, Universidad Nacional de Mar del Plata – Estación Experimental Agropecuaria Balcarce, Instituto Nacional de Tecnología Agropecuaria), CC 276 (7620), Balcarce, Argentina
[2] Consejo Nacional de Investigaciones Científicas y Técnicas (CONICET), Godoy Cruz 2290 (1425) CABA, Argentina
[3] Comisión de Investigaciones Científicas de la Provincia de Buenos Aires (CIC), CC 31 (1900) La Plata, Buenos Aires, Argentina
[4] Centro de Investigaciones de Fitopatología (CIDEFI), Facultad de Ciencias Agrarias y Forestales, Universidad Nacional de La Plata, CC 31 (1900) La Plata, Buenos Aires, Argentina

resistance factors depend on the physiological defense response of the host that affects the pathogen after infection. Passive resistance factors include morphological or developmental traits which alter conditions for infection and fungal growth development (Buerstmayr et al. 2020).

Quantitative trait loci (QTL) mapping is a useful tool for determining the genetic control behind complex traits such as resistance to FHB (Buerstmayr et al. 2020). The identification of such QTL may lead to the development of molecular markers for marker-assisted selection (MAS) and introgression and pyramidization of resistance QTL alleles, enhancing the performance against FHB in elite germplasm adapted to local conditions (Steiner et al. 2017). However, considering that plant architecture plays a significant role in disease resistance, establishing the relationship between QTL for FHB resistance and QTL for architectural traits affecting disease development becomes necessary for accelerating the development of resistant cultivars.

Several spike traits have been studied for their association with FHB resistance. However, most of the QTL mapping studies investigating the association between FHB resistance and spike morphological traits have been carried out mainly for Type I resistance. Among those, several QTL associated with resistance to initial infection have been coincident with QTL for flower opening (Zhang et al. 2018), extent of retained anthers (Buerstmayr and Buerstmayr 2015) and plant height (Buerstmayr and Buerstmayr 2016), among others. However, scarce QTL mapping studies have been carried out for ascertaining the relationship between spike architectural traits and FHB Type II resistance. A recent work carried out to investigate the association between spike morphological traits and FHB Type II resistance revealed a positive correlation between disease severity and the number of florets per spike and per spikelet (Franco et al. 2021a). These correlations may be attributed to pleiotropic effects, tightly linked genes or disease escape. A better understanding of the genetic basis of these relationships would provide useful tools to the development of FHB-resistant cultivars. Therefore, the aim of the current study was to identify QTL for FHB Type II resistance and for spike morphological traits in order to investigate these associations and enhance the current knowledge on this complex pathosystem from a breeding standpoint.

## MATERIAL AND METHODS

### Plant material

A recombinant inbred line (RIL) population, which was described in Franco et al. (2021a) and Franco et al. (2021b), was used in this study. Briefly, the population consisted of 126 lines; the parental cultivars, Baguette 10 and Klein Chajá, display medium FHB resistance level but show several differences in spike architecture.

### Phenotypic data generation

Phenotypic data used in this study were generated in a previous work (Franco et al. 2021b). Briefly, Fusarium head blight Type II resistance and spike architecture evaluations were carried out in field experiments at the INTA Balcarce Experimental Station, Buenos Aires province, Argentina, during 2016 and 2017. In each crop season, two consecutive experiments were carried out. Sowing date, sowing density and crop management were described in Franco et al. (2021a) and Franco et al. (2021b).

When each plot reached anthesis, ten flowering spikes per plot were randomly selected and inoculated using the point inoculation technique with a conidia suspension. The number of infected spikelets per spike was recorded at 12, 17 and 21 days post inoculation (dpi). FHB Severity was estimated as the proportion of infected spikelets per spike. The Area Under the Disease Progress Curve (AUDPC) was calculated, according to Shaner and Finney (1977). All the RILs and the parental cultivars were evaluated for spike morphological traits (rachis length, number of spikelets per spike, number of florets per spike and per spikelet and spike density) (Franco et al. 2021a).

### Molecular marker analysis and map construction

Of 126 RIL, 80 lines with wide phenotypic variability for all traits were randomly chosen for marker analysis. Molecular marker analysis and map construction were described in Alonso et al. (2021). Briefly, molecular genotyping was carried out with a commercial “chip”, Axiom® 35K SNP Wheat Breeder’s Array (Affimetrix) of 35.042 SNP

(single nucleotide polymorphism) markers. Only those polymorphic SNPs showing less than 10% missing data and segregation distortion under 20% were considered. The linkage map was constructed using the R/qtl software (Broman et al. 2003).

### Statistical analysis and QTL detection

Linear mixed models were fitted with the *lme* function from package *nlme* (Pinheiro et al. 2017) using R software (R Core Team 2015). Models for FHB severity 21 dpi and AUDPC traits were fitted according to Franco et al. (2021b). Models for spike morphological traits were fitted according to Franco et al. (2021a). Best linear unbiased predictors (BLUPs) were obtained for all RILs and parental cultivars, for all the variables.

Quantitative trait loci analysis was carried out using the software Windows QTL CARTOGRAPHER 2.5 (Wang et al. 2012). QTL identification was carried out by composite interval mapping (CIM) using the BLUPs of all analyzed variables. LOD ("logarithm of the odds") significance thresholds for type I error rates of α=0.1, α=0.05 and α=0.01 were determined via 500 permutations. Up to ten markers were added as cofactors in the CIM step model 6, using a moving window size of 10 centiMorgan (cM) and a walking speed of 1 cM. The most likely position of each QTL was determined as the point with the maximum LOD score. The QTL support interval criterion was defined by a LOD decrease of 2 from the maximum LOD position.

In order to test epistasis, linear models were fitted for each analyzed trait using the *lm* function in R. The models included QTL and QTL × QTL interaction effects, and BLUPs were used as phenotypic values. Quantitative trait loci main effects on the analyzed traits, the total percentage of phenotypic variance (PV) explained by each QTL and its additive effect were obtained from the model. Using the flanking sequence to each marker, provided by the chip manufacturer, a local alignment was carried out using the BLAST algorithm against the reference sequence IWGSC RefSeq v1.0 of the bread wheat genome (Appels et al. 2018) to verify its position. RIL were grouped according to the allele combination for the QTL identified (using the marker associated to the peak of maximum LOD-score for each QTL). Differences between the BLUP of these groups were compared using the Least Significant Differences (LSD) Test.

## RESULTS AND DISCUSSION

Passive resistance mechanisms include morphological and developmental traits which alter conditions for initial infection and subsequent fungal growth in the spike (Buerstmayr and Buerstmayr 2015). From this perspective, when QTL mapping studies are carried out, QTL directly responsible for FHB resistance need to be clearly differentiated from those for spike architecture traits indirectly affecting *Fusarium* infection and spread. This is important for breeders in order to prevent the concomitant introgression of certain morphological traits along with FHB resistance (by means of pleiotropy, linkage or even false QTL detection) into an elite variety (Buerstmayr et al. 2020). In a previous work carried out in the same RIL population as the one used here (Franco et al. 2021b), FHB Type II resistance was evaluated; in parallel, several spike traits which might alter the fungus colonization were evaluated and some of them were found to be significantly associated with FHB resistance: FHB severity 21 dpi and AUDPC were positively correlated (P<0.05) with the number of florets per spike and with the number of florets per spikelet (Supplementary Table 1). In the present study, a QTL mapping was carried out in order to further investigate these associations and gain insight into the genetic control of this complex disease.

***Table 1.*** Chromosomal location [chromosome (Chrom.), closest marker and flanking markers], additive effect (Add), LOD score and percentage of phenotypic variance (PV) explained by the three QTL detected for both FHB severity 21 dpi and AUDPC

| | | | Severity 21 dpi[c] | | | AUDPC[d] | | |
|---|---|---|---|---|---|---|---|---|
| Chrom. | **Closest marker** | **Flanking markers** | **Add[a]** | **LOD** | **%PV[b]** | **Add[a]** | **LOD** | **%PV[b]** |
| 2A | *AX-94406147* (L2A7) | *AX-94639168* (L2A5) - *AX-94438643* (L2A9) | -0.2 | 2.9 | 2.9 | -0.2 | 6.0 | 3.6 |
| 4A | *AX-94767736_4A* (L4A14) | *AX-94503294* (L4A13) - *AX-94767736_4A* (L4A14) | -0.3 | 6.8 | 16.0 | -0.3 | 8.6 | 18.2 |
| 6D | *AX-95130119* (L6D4) | *AX-94532403* (L6D3) - *AX-95120751* (L6D7) | -0.2 | 3.8 | 2.6 | -0.2 | 5.9 | 2.4 |

[a] Additive effect; a negative value indicates that the Baguette 10 allele decreases the trait BLUP as compared with that of the Klein Chajá allele. [b] Percentage of phenotypic variance explained by the QTL. [c] Permutation test for severity 21 dpi BLUPs, 500 iterations: α 0.1 = 2.9, α 0.05 = 3.2, α 0.01 = 4.1. [d] Permutation test for AUDPC BLUPs, 500 iterations: α 0.1 = 3.1, α 0.05 = 3.4, α 0.01 = 4.1

The RIL population evaluated showed large genetic variation and transgressive segregation for both FHB Type II resistance and spike architecture traits (Supplementary Figure 1) across all environments; in addition, high heritability values were obtained for all these traits (Supplementary Table 2), indicating that a large proportion of the variation among the lines was due to genetic effects, particularly considering the wide array of environmental conditions (Franco et al. 2021a). These results give further validity to the QTL detection process carried out in the present study.

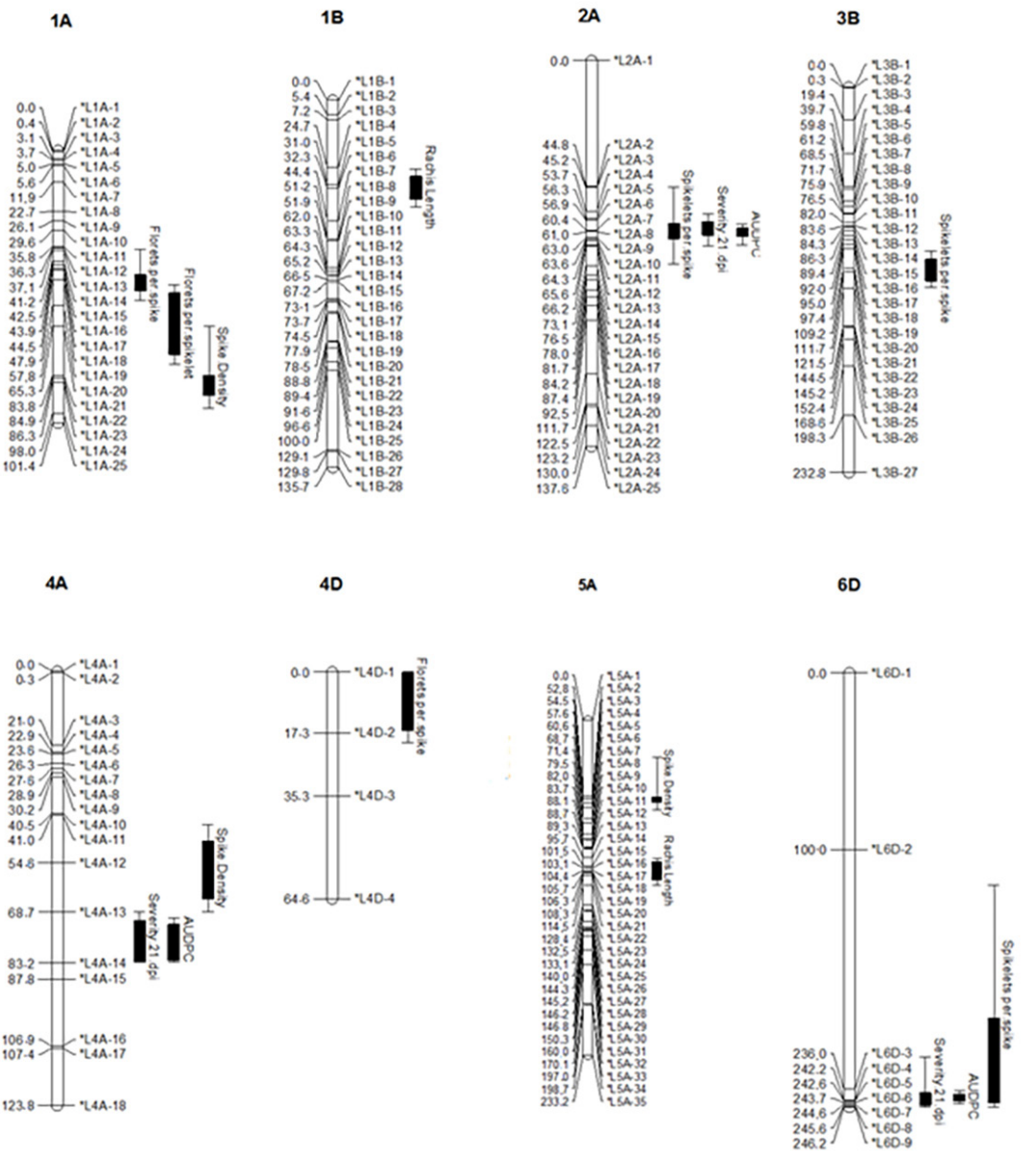


***Figure 1.*** Linkage map and positions of QTL for FHB severity 21 dpi, AUDPC and spike architecture traits detected in the Baguette 10/ Klein Chajá RIL population (N=80) evaluated in four experiments at Balcarce, Argentina. Best linear unbiased predictors (BLUP) were used in QTL mapping. A black vertical box represents a LOD decrease of 1.0 from the peak LOD value at each QTL. Error bar indicates an LOD drop of 2.0 from the peak LOD value at each QTL.

***Table 2.*** Chromosomal location [chromosome (Chrom.), closest marker and flanking markers], additive effect (Add), LOD score and percentage of phenotypic variance (PV) explained by QTL detected for morphological spike traits

| Trait | Chrom. | Closest marker | Flanking markers | Add[a] | LOD | %PV[b] |
|---|---|---|---|---|---|---|
| Spike density[c] | 1A | AX-94910420 (L1A22) | *AX-94750566* (L1A20) - *AX-94402351* (L1A24) | -0.06 | 2.8 | 2.6 |
| | 4A | *AX-94977239* (L4A12) | AX-95631864 (L4A10) - *AX-94760290* (L4A13) | 0.05 | 3.8 | 3.8 |
| | 5A | AX-94909932 (L5A2) | *AX-94909932* (L5A2) - *AX-94432552* (L5A4) | 0.06 | 3.5 | 2.0 |
| Rachis length[d] | 1B | *AX-94861978* (L1B5) | *AX-95190390_1B* (L1B4) - *AX-94592974* (L1B7) | 0.22 | 4.3 | 3.9 |
| | 5A | *AX-94927881* (L5A17) | *AX-94731078_5A* (L5A14)- *AX-94667285* (L5A21) | -0.33 | 3.5 | 10.5 |
| Spikelets per spike[e] | 2A | *AX-94406147* (L2A7) | *AX-94639168* (L2A5) - *AX-94438643* (L2A9) | 0.49 | 3.3 | 9.4 |
| | 3B | *AX-94587694* (L3B19) | *AX-94810838* (L3B18) - *AX-95233557* (L3B21) | 0.62 | 3.4 | 1.3 |
| | 6D | *AX-94532403* (L6D3) | *AX-95114964* (L6D2) - *AX-95130119* (L6D4) | -0.54 | 3.6 | 6.0 |
| Florets per spike[f] | 1A | AX-94802893 (L1A18) | AX-94889305_1A (L1A16) - AX-95137011 (L1A19) | -1.27 | 2.9 | 5.9 |
| | 4D | *AX-95257633* (L4D1) | *AX-95257633* (L4D1) - *AX-94740564* (L4D2) | -2.15 | 6.8 | 14.1 |
| Florets per spikelet[g] | 1A | *AX-95137011* (L1A19) | *AX-94802893* (L1A18) - *AX-94552630* (L1A20) | -0.13 | 4.3 | 6.2 |
| | 5D | *AX-94863307* (L5D2) | *AX-94938800* (L5D1) - *AX-94397264* (L5D4) | 0.11 | 4.6 | 3.1 |

[a] Additive effect; a negative value indicates that the Baguette 10 allele decreases the trait BLUP as compared with that of the Klein Chajá allele. [b] Percentage of phenotypic variance explained by the QTL. [c] Permutation test for Spike density over BLUPS, 500 iterations: α 0.1 = 2.6, α 0.05 = 2.9, α 0.01 = 3.3. [d] Permutation test for Rachis length over BLUPS, 500 iterations: α 0.1 = 2.8, α 0.05 = 3.1, α 0.01 = 3.8. [e] Permutation test for Spikelets per spike over BLUPS, 500 iterations: α 0.1 = 2.8, α 0.05 = 3.1, α 0.01 = 3.8. [f] Permutation test for Florets per spike over BLUPS, 500 iterations: α 0.1 = 2.9, α 0.05 = 3.1, α 0.01 = 4.3. [g] Permutation test for Florets per spikelet over BLUPS, 500 iterations: α 0.1 = 2.9, α 0.05 = 3.1, α 0.01 = 4.1.

Results of molecular marker analysis and map construction were described in Alonso et al. (2021). As discussed by these authors, very stringent conditions were applied to the map construction and QTL mapping procedures, in order to overcome the limitations of the use of a population of reduced size. Briefly, the map consisted of 368 loci on the 21 chromosomes of bread wheat (Supplementary Table 3).

Composite interval mapping identified three significant QTL associated with both FHB severity 21 dpi and AUDPC. In the three regions, the co-localization of QTL for FHB severity 21 dpi and AUDPC can be explained by the high genetic correlation found between these traits (r=0.94; Franco et al. 2021a), which is consistent with data reported by Buerstmayr and Buerstmayr (2016). These QTL mapped respectively on chromosomes 2A, 4A and 6D, their position and statistical parameters are presented in Table 1. Only QTL with LOD values greater than the LOD significance threshold and significant in the linear model analysis are presented. Linkage groups and confidence intervals of QTL are shown in Figure 1. For all three QTL, the allele improving the resistance level was derived from the donor parent Baguette 10.

The effects of individual QTL were variable. The QTL with the largest effect explained 16% and 18.2% of the phenotypic variance for FHB severity 21 dpi and AUDPC, respectively. This QTL was mapped on chromosome 4A, within a 14.3 cM interval for FHB severity 21 dpi and 12.5 cM interval for AUDPC, with the peak marker close to *AX-94767736_4A*. In a similar study carried out under greenhouse conditions, a significant QTL for Type II resistance was identified at this location linked to the marker *wsnp_JD_c27162_22206547* (Zhang et al. 2018). This marker was mapped within the confidence interval of the QTL detected in the present study. At the level of resolution afforded by this mapping study, we cannot distinguish whether they are the same or different QTL.

The second QTL, on chromosome 2A, was mapped close to *AX-94406147* and explained 2.9% and 3.6% of the PV for FHB severity 21 dpi and AUDPC, respectively. Several authors have reported QTL for the same trait on that genomic region in different wheat cultivars: (1) 'Ning7840', derived from 'Sumai 3', associated with marker *Xgwm614* (Zhou et al. 2002); (2) 'Ning8026', 'Wangshuibai' and 'Spark' close to marker *Xgwm515* near the centromere (Gosman et al. 2008); and (3) 'Stoa' and 'Arina', on the distal part of chromosome 2A, close to marker *XksuH16* (Waldron et al. 1999). The QTL found in this study is closely linked to the marker *Xgwm328*, which is associated with the QTL in 'Ning8026', 'Wangshuibai' and 'Spark'. Further studies are needed to determine whether they are the same or different QTL.

The third QTL, on the distal end of chromosome 6D, was mapped close to *AX-95130119* and accounted for 2.6% and 2.4% of the PV for FHB severity 21 dpi and AUDPC, respectively. To date, the only QTL detected in this position was reported by Holzapfel et al. (2008), close to the marker *Xbarc96* for FHB Type I resistance. In this way, our study constitutes the first report of a QTL associated with Type II resistance to FHB in this region. The possibility that it is

the same QTL controlling somehow both types of resistance is not discarded. Considering that the level of resolution achieved with this mapping study does not allow distinguishing whether both QTL are the same or different, the QTL for type II resistance identified in the present study needs to be further investigated with respect to its relation to the QTL reported by Holzapfel et al. (2008).

Together, the three significant QTL explained 39.5% of the PV for FHB severity 21 dpi and 37.6% for AUDPC. No significant epistatic QTL interactions were detected, showing that QTL effects were mostly additive. Substantial variation in environmental conditions between experiments was observed (Franco et al. 2021a, Franco et al. 2021b); however, QTL were detected using BLUPs as phenotypic data, which represent only the genetic value of each individual. Despite the existence of transgressive segregation in the population, it was not possible to detect significant QTL in which the parental cultivar Klein Chajá contributed the favorable allele. This was likely caused by the relatively low number of individuals of the mapping population and/or by the fact that these QTL were of minor effect. It is known that the use of mapping populations of reduced size, as was the case in the present study, provides power to detect QTL with major effects, but limits the detection of additional, small, yet real QTL (Cavalcanti et al. 2012). In this context, Schön et al. (2004) recommend the use of a conservative threshold, such as the one used in this study, if the aim is to identify a few large QTL controlling a limited proportion of the genetic variance.

The eight possible allele combinations for the three QTL found in this study were detected in the population (Figure 2). The genotypes with the three favorable alleles (Allele combination 1), derived from Baguette 10 (*B* alleles), occurred in 1.4% of the RIL population. This combination significantly improved FHB Type II resistance, respectively reducing the mean FHB severity 21 dpi and AUDPC by 35.2% and 37.7% compared to the combination with the three non-favorable alleles, derived from Klein Chajá (Allele combination 8); moreover, the decrease in the average trait values encompassed the increase in the number of favorable alleles. This may be promising in the context of genetic improvement for FHB Type II resistance; however, Baguette 10, the donor of these favorable alleles, showed less Type II resistance than the RIL with the same allelic constitution for the QTL under study. Therefore, further studies are needed to understand the

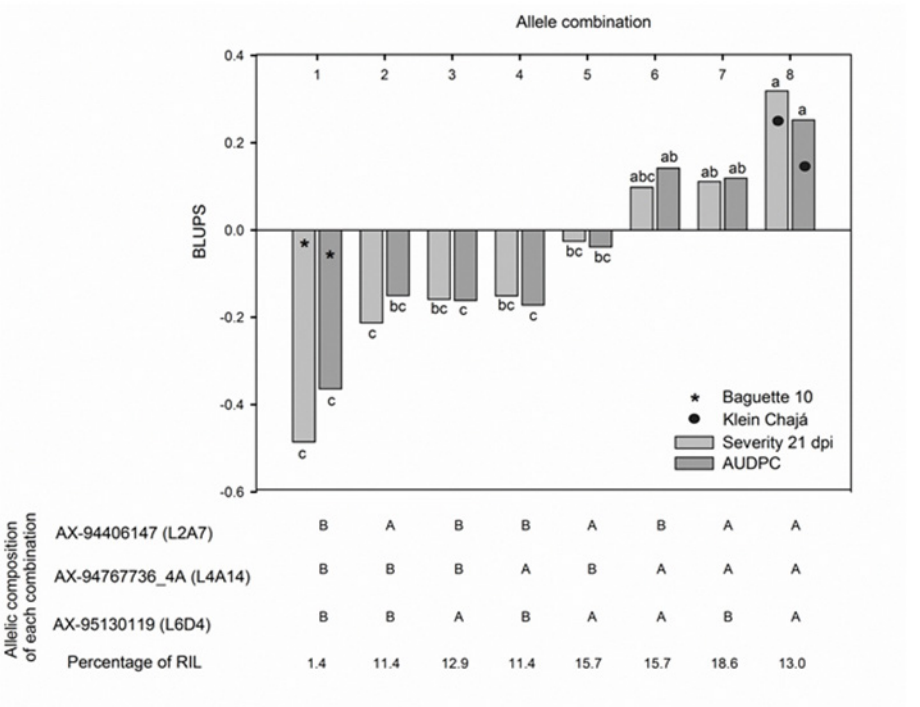


***Figure 2.*** Mean of best linear unbiased predictors (BLUP) for severity 21 dpi and AUDPC for each allele combination for the three QTL detected in the Baguette 10/Klein Chajá RIL population. The allelic composition and the percentage of RILs of each allele combination are shown at the bottom; A: allele derived from Klein Chajá; B: allele derived from Baguette 10.

usefulness of these QTL in breeding for FHB resistance.

Considering the passive component of the resistance to FHB, QTL were detected for spike density, number of spikelets per spike, number of florets per spike, number of florets per spikelet and rachis length. Chromosomal location and estimates of QTL effects are summarized in Table 2. Only QTL exceeding the LOD significance threshold and significant in the linear model are presented. Linkage groups and position of QTL are shown in Figure 1.

To date, spike density has been one of the most extensively studied variables in wheat and other species due to its association with FHB resistance (Huang et al. 2018, Jones et al. 2018). Several studies argue that genotypes with denser spikes have a faster disease spread because the density may facilitate pathogen spread to adjacent nodes or due to the microclimate conditions that are generated in the denser spikes (Buerstmay et al. 2011). In this population, spike density was not associated with Type II resistance to FHB. These results were in agreement with Buerstmayr et al. (2012), who showed variable associations between these traits depending on the population studied. From the QTL mapping three genomic regions affecting spike density were detected. These were located on chromosomes 1A, 4A and 5A. The individual QTL had generally low effect and contributed between 2% and 3.8% to the PV. None of the detected QTL for this trait overlapped with QTL for FHB resistance, coinciding with Buerstmayr et al. (2012). However, the QTL on chromosome 4A mapped very close to the QTL for FHB severity 21 dpi and AUDPC. In this context, Zhang et al. (2018) found overlapping of QTL for FHB resistance and QTL for spike density near this region. In short, whether there is a functional association between spike density and FHB type II resistance remains to be ascertained.

Few investigations have studied the association between rachis length and type II resistance to FHB. Some studies, such as the one carried out by Somers et al. (2003), have reported lack of correlation between these variables, suggesting that this morphological trait does not constitute a passive resistance factor to FHB. In this population two QTL were associated with rachis length on the chromosomes 5A and 1B. None of these QTL overlapped with FHB Type II resistance QTL, coinciding with Somers et al. (2003). On the other hand, a study carried out by Buerstmayr et al. (2011) found co-localization between QTL for FHB resistance and rachis length on chromosome 5A. However, they concluded that such co-localization was rather due to linkage than pleiotropy. In this way, the lack of correlation between these traits and of QTL co-localization in this population suggests that these characters are under different genetic control.

For the number of spikelets in the spike, three QTL located on chromosomes 2A, 3B and 6D were detected. The QTL for number of spikelets in the spike on chromosome 2A co-localized with QTL for FHB severity 21 dpi and AUDPC. Plants carrying the Baguette 10 allele at this location were more resistant to FHB and showed spikes with higher number of spikelets. Surprisingly, co-localization of QTL for FHB Type II resistance and number of spikelets per spike was also found on chromosome 6D, near marker *AX-94532403*, with the Baguette 10 allele increasing the level of Type II resistance to FHB and reducing the number of spikelets in the spike. This overlapping of QTL may be due to close linkage or pleiotropic effect. However, at the level of map resolution achieved in this research, the two cannot be unambiguously distinguished. Additional fine-mapping studies are required to determine if the co-localizations between these QTL are due to linkage or pleiotropy. This overlapping of QTL may underlie an influence of this morphological trait on the spread of the fungus in the spike. However, despite the co-localization, this spike attribute was not correlated either with FHB severity 21 dpi or AUDPC coinciding with Buerstmayr et al. (2011). Presumably, this lack of correlation could be due to the low percentage of PV for FHB type II resistance explained by these two QTL.

Finally, two moderate-effect QTL associated with the number of florets per spike were found on chromosomes 1A and 4D, none of which overlapped with QTL for FHB Type II resistance. In the same manner, the two minor-effect QTL for number of florets per spikelet found on chromosomes 1A and 5D did not coincide with QTL for FHB resistance. Considering the positive genetic correlation found between the number of florets per spike and per spikelet with FHB severity 21 dpi and AUDPC (Franco et al. 2021a) and the lack of overlapping between these QTL, these spike morphological traits possibly act as passive resistance factors to FHB in wheat. It is likely that a higher number of florets provide a microclimate of high humidity in the spike, favoring the fungal sporulation and its spread within the spike. Likewise, it may provide greater inoculum pressure in the rachis node benefiting the spread of the fungus in the spike and the disease development. In summary, spike architecture traits -notably, the number of florets per spike and per spikelet - should be taken into consideration in the design of breeding strategies to increase Type II resistance to FHB in bread wheat.

## ACKNOWLEDGMENTS

We thank members of the Grupo Trigo Balcarce (INTA BAlcarce) for helping with the experiments. Scholarships granted to M.F. Franco and M.P. Alonso by the CONICET and partial funding from INTA (grant no. PNCyO 1127044) are acknowledged. Supplementary files are available with the corresponding author.

## REFERENCES

Alonso MP, Vanzetti LS, Crescente JM, Mirabella NE, Panelo JS and Pontaroli AC (2021) QTL mapping of spike fertility index in bread wheat. **Crop Breeding and Applied Biotechnology 21**: e34402113.

Appels R, Eversole K, Stein N, Feuillet C, Keller B, Rogers J, Pozniak CJ, Choulet F, Distelfeld A and Poland J (2018) Shifting the limits in wheat research and breeding using a fully annotated reference genome. **Science 361**: 1-13.

Bai G, Su Z and Cai J (2018) Wheat resistance to Fusarium head blight. **Canadian Journal of Plant Pathology 40**: 336-346.

Broman K, Wu H, Sen S and Churchill G (2003) R/qtl: qtl mapping in experimental crosses. **Bioinformatics 19:** 889-890.

Buerstmayr M and Buerstmayr H (2015) Comparative mapping of quantitative trait loci for *Fusarium* head blight resistance and anther retention in the winter wheat population Capo × Arina. **Theoretical and Applied Genetics 128**: 1519-1530.

Buerstmayr M and Buerstmayr H (2016) The semidwarfing alleles Rht-D1b and Rht-B1b show marked differences in their associations with anther-retention in wheat heads and with Fusarium head blight susceptibility. **Phytopathology 106:** 1544-1552.

Buerstmayr M, Huber K, Heckmann J, Steiner B, Nelson JC and Buerstmayr H (2012) Mapping of QTL for *Fusarium* head blight resistance and morphological and developmental traits in three backcross populations derived from *Triticum dicoccum* x *Triticum durum*. **Theoretical and Applied Genetics 125**: 1751-1765.

Buerstmayr M, Lemmens M, Steiner B and Buerstmayr H (2011) Advanced backcross QTL mapping of resistance to Fusarium head blight and plant morphological traits in a *Triticum macha* × *T. aestivum* population. **Theoretical and Applied Genetics 123:** 293.

Buerstmayr M, Steiner, B and Buerstmayr H (2020) Breeding for Fusarium head blight resistance in wheat - Progress and challenges. **Plant Breeding 139**: 429-454.

Cavalcanti JJV, Santos FHC, Silva FP and Pinheiro CR (2012) QTL detection of yield-related traits of cashew. **Crop Breeding and Applied Biotechnology 12:** 60-66.

CIMMYT - Centro Internacional de Mejoramiento de Maíz y Trigo (2019) Available at <https://www.cimmyt.org/news/food-security/>. Accessed on September 15, 2020.

Ferrigo D, Raiola A and Causin R (2016) Fusarium toxins in cereals: Occurrence, legislation, factors promoting the appearance and their management. **Molecules 21**: 627.

Franco MF, Lori GA, Cendoya MG, Alonso MP, Panelo JS, Malbrán I, Mirabella NE and Pontaroli AC (2021a) Spike architecture traits associated with type ii resistance to Fusarium head blight in bread wheat. **Euphytica 217**: 1-2.

Franco MF, Lori GA, Panelo J, Alonso M, NE M, Malbrán I, Cendoya M and Pontaroli AC (2021b) Using anthesis date as a covariate to accurately assessing Type II resistance to Fusarium head blight in field-grown bread wheat. **Crop Protection 142**: 1-10.

Gosman N, Steed A, Simmonds J, Leverington-Waite M, Wang Y, Snape J and Nicholson P (2008) Susceptibility to Fusarium head blight is associated with the Rht-D1b semi-dwarfing allele in wheat. **Theoretical and Applied Genetics 116**: 1145-1153.

Holzapfel J, Voss H, Miedaner T, Korzun V, Haberle J, Schweizer G, Mohler V, Zimmermann G and Hartl L (2008) Inheritance of resistance to *Fusarium* head blight in three European winter wheat populations. **Theoretical and Applied Genetics 117**: 1119-1128.

Huang Y, Haas M, Heinen S, Steffenson BJ, Smith KP and Muehlbauer GJ (2018) QTL mapping of fusarium head blight and correlated agromorphological traits in an elite barley cultivar Rasmusson. **Frontiers in plant science 9:** 1260.

Jones S, Farooqi A, Foulkes J, Sparkes DL, Linforth R and Ray RV (2018) Canopy and ear traits associated with avoidance of Fusarium head blight in wheat. **Frontiers in Plant Science 9:** 1021.

Mesterhazy A (2020) Updating the breeding philosophy of wheat to Fusarium head blight (FHB): Resistance components, QTL identification, and phenotyping - a review. **Plants 9:** 1702.

Mielniczuk E and Skwaryło-Bednarz B (2020) Fusarium head blight, mycotoxins and strategies for their reduction. **Agronomy 10**: 509.

Pinheiro J, Bates D, DebRoy S, Sarkar D, Heisterkamp S, Van Willigen B and Maintainer R (2017) Package 'nlme'. Linear and nonlinear mixed effects models, version, 3.1. Available at <https://svn.r-project.org/R-packages/trunk/nlme/>. Accessed on October 4, 2020.

R Core Team (2015) R: A language and environment for statistical computing. R Foundation for statistical computing, Vienna. Available at <https://www.r-project.or g/>. Accessed on October 14, 2020.

Schön C, Utz H, Groh S, Truberg B, Openshaw S and Melchinger A (2004) Quantitative trait locus mapping based on resampling in a vast maize testcross experiment and its relevance to quantitative genetics for complex traits. **Genetics and Molecular Biology 167:** 485-498.

Shaner G and Finney R (1977) The effect of nitrogen fertilization on the expression of slow-mildewing resistance in Knox wheat. **Phytopathology 67**: 1051-1056.

Somers DJ, Fedak G and Savard M (2003) Molecular mapping of novel genes controlling Fusarium head blight resistance and deoxynivalenol

accumulation in spring wheat. **Genome 46:** 555-564.

Steiner B, Buerstmayr M, Michel S, Schweiger W, Lemmens M and Buerstmayr H (2017) Breeding strategies and advances in line selection for Fusarium head blight resistance in wheat. **Tropical Plant Pathology 42**: 165-174.

Waldron B, Moreno-Sevilla B, Anderson J, Stack R and Frohberg R (1999) RFLP mapping of QTL for Fusarium head blight resistance in wheat. **Crop Science 39**: 805-811.

Wang S, Basten CJ and Zeng ZB (2012) Windows QTL cartographer 2.5. North Carolina State University, Department of Statistics, Raleigh. Available at <http://statgen.ncsu.edu/qtlcart/WQTLCart.htm>. Accessed on November 7, 2020.

Zhang W, Francis T, Gao P, Boyle K, Jiang F, Eudes F, Cuthbert R, Sharpe A and Fobert PR (2018) Genetic characterization of Type II Fusarium head blight resistance derived from transgressive segregation in a cross between Eastern and Western Canadian spring wheat. **Molecular Breeding 38**: 1-18.

Zhou W, Kolb FL, Bai G, Shaner G and Domier LL (2002) Genetic analysis of scab resistance QTL in wheat with microsatellite and AFLP markers. **Genome 45**: 719-727.